Accepted Manuscript

Synthesis, properties and quantum chemical evaluation of solvatochromic pyridinium-phenyl-1,3-thiazol-4-olate betaine dyes

Roberto Menzel, Stephan Kupfer, Ralf Mede, Helmar Görls, Leticia González, Rainer Beckert

PII: S0040-4020(12)01846-7

DOI: 10.1016/j.tet.2012.12.016

Reference: TET 23828

To appear in: *Tetrahedron*

Received Date: 22 October 2012

Revised Date: 27 November 2012

Accepted Date: 7 December 2012

Please cite this article as: Menzel R, Kupfer S, Mede R, Görls H, González L, Beckert R, Synthesis, properties and quantum chemical evaluation of solvatochromic pyridinium-phenyl-1,3-thiazol-4-olate betaine dyes, *Tetrahedron* (2013), doi: 10.1016/j.tet.2012.12.016.

iGraphical Abstract

To create your abstract, type over the instructions in the template box below.
Fonts or abstract dimensions should not be changed or altered.

Synthesis, properties and quantum chemical evaluation of solvatochromic pyridinium-phenyl-1,3-thiazol-4-olate betaine dyes

Roberto Menzel, Stephan Kupfer, Ralf Mede, Helmar Görls, Leticia González, Rainer Beckert

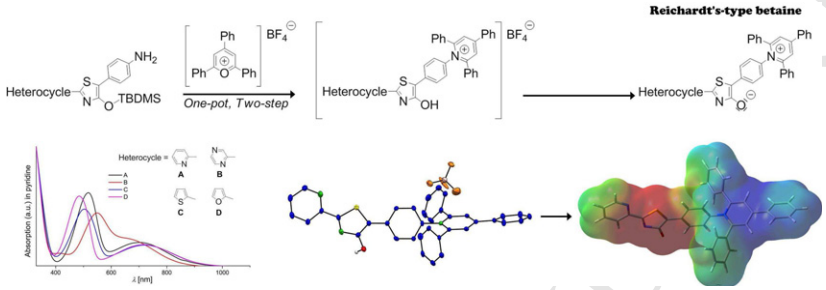

Tetrahedron
journal homepage: www.elsevier.com

Synthesis, properties and quantum chemical evaluation of solvatochromic pyridinium-phenyl-1,3-thiazol-4-olate betaine dyes

Roberto Menzel [a], Stephan Kupfer [b, c], Ralf Mede [a], Helmar Görls [d], Leticia González [c*], Rainer Beckert [a*]

[a] *Friedrich Schiller University Jena, Institute of Organic and Macromolecular Chemistry, Humboldtstraße 10, 07743 Jena, Germany.*
[b] *Friedrich Schiller University Jena, Institute of Physical Chemistry, Helmholtzweg 4, 07743 Jena, Germany.*
[c] *University of Vienna, Institute of Theoretical Chemistry, Waehringer Str. 17, 1090 Vienna, Austria.*
[d] *Friedrich Schiller University Jena, Institute of Inorganic and Analytical Chemistry, Humboldtstraße 8, 07743 Jena, Germany.*

ARTICLE INFO

Article history:
Received
Received in revised form
Accepted
Available online

Keywords:
4-Hydroxy-1,3-thiazoles
Betaine dyes
Solvatochromism
Donor-acceptor system
Linear solvation energy relationship (LSER)

ABSTRACT

The syntheses and characterizations of four zwitterionic betaines are presented. These dyes possess an uncommon heterocyclic 1,3-thiazol-4-olate donor moiety. The natures of the HOMO/LUMO transitions and of the intramolecular charge-transfer state were assigned with the help of quantum chemical calculations. Multiple intermolecular solute/solvent interactions were discussed using linear solvation energy relationship (LSER) with Kamlet-Taft and Catalán parameters. The dyes show a pronounced negative solvatochromism ranging from λ_{max} 392 nm in TFE to 820 nm in THF ($\Delta\lambda$ = 428 nm or 1.65 eV). The X-ray structures of one of the tetrafluoroborate salts and of one of the betaines are discussed.

1. Introduction

Compounds of the class of pyridinium *N*-phenolates are widely used as solvatochromic, thermochromic, piezochromic and halochromic functional dyes.[1] After the first synthesis of 2,6-diphenyl-4-(2,4,6-triphenylpyridinio)phenolate (*Reichardt's dye*, **30**, Figure 1) in 1963,[2] the empirical parameter of solvent polarity, the E_T(**30**) values, were established to develop the E_T(**30**) and normalized E_T^N(**30**) solvent polarity scale. The E_T(**30**) values are simply defined as the molar electronic transition energies of the Reichardt's dye, measured in solvents with different polarity.[3] The number **30** simply comes from Dimroth´s and Reichardt´s randomly chosen reference number of the dye in the first publication. Since then, several different derivatives have been synthesized and several publications and reviews have been published to explore and explain the characteristics of these compounds.[4-6] Numerous betaines were classified in a research article from Dominguez and Rezende in 2010.[7] Additionally, they tried to give a rationalized view to estimate whether a betaine (also other dyes) exhibits a negative, inverted or positive solvatochromism.[8] Because of their unique spectroscopic properties, they can and are used mainly to measure solvent polarity of pure solvents and binary solvent mixtures,[9-11] to describe the solvent properties of ionic liquids,[12] as polarity and acid-base responsible dyes for molecular recognition,[13] as optical alcohol sensors in polymer membranes,[14] to examine the electrophilicity of lanthanide shift reagents,[15] to determine alterations in micellar structures,[16] and, very recently, as probes to determine the degree of substitution in cellulose derivatives.[17]

The majority of the Reichardt's-type betaine dyes consist of *N*-phenolate donor moieties and only few examples are known which possess an unconventional purinolate or barbiturate-based one.[18] We choose the 4-hydroxy-1,3-thiazole core as an alternative to the *N*-phenolate group in order to extend the scope of available donor-acceptor betaine dyes. To the best of our knowledge, this is the first example where the anionic compartment not only acts as the electron donor, but also as the chromophore itself. The class of the 4-hydroxy-1,3-thiazoles was recently revived by our group due to their outstanding chemical and optical properties and, additionally, they allow an easy chemical functionalization toward the application desired. They have already been used as dyes in polymers, *e.g.* in a terpolymer as a FRET energy donor combined with a Ru(II) complex as the acceptor unit,[19] as sensitizers in Grätzel-type dye-sensitized solar cells (DSSCs),[20] and furthermore, as specific sensor molecules for the detection of fluoride ions,[21] or as light-harvesting ligands

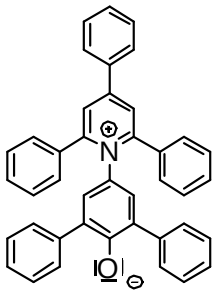

Figure 1. Structure of the Reichardt's betaine **30** used as reference compound in this study

∗ Corresponding author. Tel.: +49-3641-9-48230; fax: +49-3641-948212; e-mail: c6bera@uni-jena.de

in Ru(II)-polypyridyl complexes.[22,23] They can easily be equipped with various functional groups. Especially the facile introduction of acceptor or donor moieties makes them suitable for the construction of betaine dyes which possess a thiazol-4-olate as donor and a pyridinium as acceptor group. Therefore, several donor-acceptor dyes consisting of a 1,3-thiazole core, a triphenyl pyridinium group and a heterocycle in the 2-position at the thiazole (pyridinyl, pyrazinyl, thiophenyl and furanyl) to vary the electronic and physical (solubility) properties of the betaines have been synthesized. Additionally, the solid state structures of one of the tetrabutylammonium salts and of one of the betaines derived are provided.

2. Results and Discussions

2.1. Synthesis

The synthetic route and the structures of the betaine dyes are depicted in Scheme 1. In a first step, the starting materials **1a**-**1d** were synthesized by a Hantzsch cyclization reaction of the corresponding thioamide with ethyl 2-bromo-2-(4-nitrophenyl)-acetate.[23] Several attempts to reduce the nitro group to the amine, starting directly from the 4-hydroxy-1,3-thiazoles, resulted in a hardly separable mixture (due to the very poor solubility of **1a**-**1d**) and to a very sluggish conversion of the starting material. Therefore, the hydroxy group of the 4-hydroxy-1,3-thiazoles was protected as silyl ether by reacting with *tert*-butyldimethylsilyl chloride (TBDMSCl), which facilitated the work up process dramatically. Reduction was carried out with Pd/C and H_2 (10 bar) in an autoclave with MeOH or THF as the solvent in good to very good yields (75-88%). We also used hydrazine hydrate and Raney nickel in test reactions which, unexpectedly, led to a more or less desilylation back to the 4-hydroxy-1,3-thiazoles and only to a poor formation of the products desired. The transformation of the amines to the pyridinium salts was carried out as a one-pot (ANRORC) reaction. Firstly, a vinylogous amide, catalyzed with Et_3N (1 equiv), is formed in a ring opening sequence between the 2,4,6-triphenylpyrylium tetrafluoroborate and the corresponding aryl amine;[24] secondly, the ring closure is achieved by heating the resulting black mixture with a twofold excess of AcOH (2 equiv) in EtOH (96%) under reflux and, thirdly, the silyl ether is cleaved under the acidic conditions used. The tetrafluoroborate salts synthesized were deprotonated with tetrabutylammonium hydroxide (TBAOH) in MeOH in order to obtain the "free" betaines almost quantitatively (the process is fully reversible and other salts can be obtained).

2.2. X-ray structure of 4a and C.

Crystals of the tetrafluoroborate salt **4a** suitable for X-ray structure analysis were obtained by adding acetone directly to the hot reaction mixture till the product dissolved followed by slowly cooling down to r.t. One molecule of the compound crystallizes together with one molecule of ethanol in light yellow crystals. The structure and data are depicted in Figure 2 (additional refinement data is reported in the ESI S1). Two of the molecules of **4a** are connected with one solvent molecule ethanol which forms two medium-strength hydrogen bonds, one from the hydrogen of the hydroxy group of the thiazole [O1-O1E 2.562(6) Å] and one to the pyridine nitrogen from the hydroxy group of the ethanol [O1E-N1 2.814(7) Å]. The phenyl rings at the pyridinium core are twisted out of planarity due to steric hindrance [*e.g.* N3-C19-C20-C25 59.06(4) °], as described for various similar triphenylpyridinium derivatives.[25-27] The phenyl and pyridyl ring connected to the thiazole also are twisted to some extent [C7-C8-C9-C14 25.97(5) ° and S1-C6-C5-N1 24.98(2) °]. There are no dispersive interactions among the two molecules as the distance between their aromatic rings is too far. The bond lengths and angles of the (hetero)aryl rings and of the thiazole, with the sulfur in an almost perpendicular arrangement due to the missing hybridization, are all in the expected range.[28]

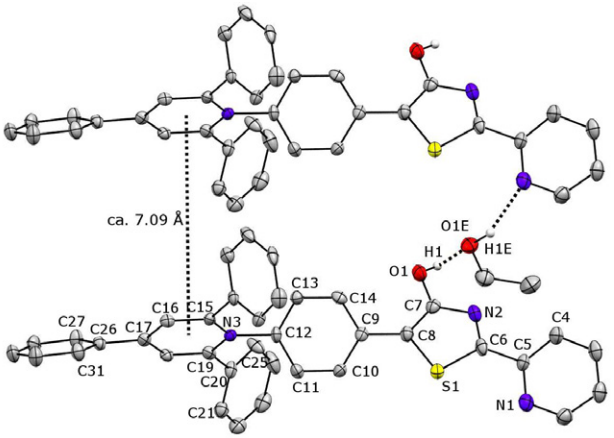

Figure 2. ORTEP plot and numbering scheme of **4a**. Ellipsoid probability is 50%. Hydrogen atoms (except the calculated atoms of the hydrogen bonds) and counter ions are omitted. Selected bond lengths (Å) and angles (°) are: S1-C6 1.733(6), C6-N2 1.316(8), N2-C7 1.369(7), C7-C8 1.384(8), C8-S1 1.731(6), C7-O1 1.350(7), C6-C5 1.471(8), C8-C9 1.460(8), C5-N1 1.343(8), N3-C12 1.478(8), S1-C6-N2 114.7(4), C6-N2-C7 109.9(5), N2-C7-C8 117.5(5), C7-C8-S1 107.6(4), C8-S1-C 90.3(3), C7-C8-C9-C14 25.97 (5), S1-C8-C9-C10 26.12(3), S1-C6-C5-N1 24.98(2), N2-C6-C5-C4 20.92(4), C13-C12-N3-C15 69.48(4), N3-C19-C20-C25 59.06(4), C16-C17-C26-C27 143.04(6).

X-ray structures of Reichardt's betaines are rare in this field and only few examples are known.[25,29,26] Crystals of compound **C** were obtained after various attempts by slow diffusion of MeOH into DMSO. Therefore, a solution of **C** in DMSO was covered with a layer of MeOH directly in an NMR tube which yielded deep violet very thin needles. The compound crystallized as a solvate together with one molecule of MeOH and one molecule of water. Both solvent molecules form strong hydrogen bonds [O1-O1E 2.806(7) Å and O1-O1W 2.690(9) Å] to the thiazole oxygen O1. The structure and data are depicted in Figure 3 (additional refinement data is reported in the ESI S1). The pyridinium moiety features a similar geometry like **4a**. The phenyl rings are twisted out of the pyridinium plane [*e.g.* N3-C19-C20-C25 66.23(5) °] to a greater extent probably because of the reduced bond length between N3 and C12 [1.462(8) Å instead of 1.478(8) Å] leading to an enhanced steric hindrance.

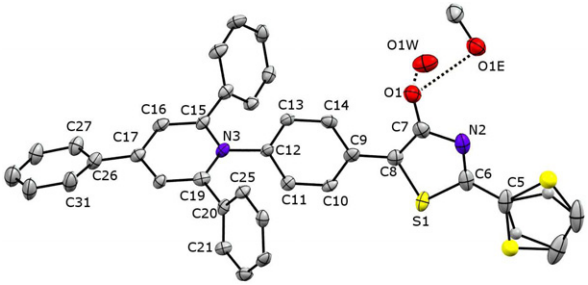

Figure 3. ORTEP plot and numbering scheme of **C**. Ellipsoid probability is 50%. Hydrogen atoms are omitted. Selected bond lengths (Å) and angles (°) are: S1-C6 1.726(7), C6-N2 1.309(9), N2-C7 1.428(10), C7-C8 1.396(10), C8-S1 1.752(7), C7-O1 1.278(8), C8-C9 1.405(9), N3-C12 1.462(8), S1-C6-N2 116.0(6), C6-N2-C7 110.5(6), N2-C7-C8 114.2(7), C7-C8-S1 109.2(5), C8-S1-C 90.1(4), C7-C8-C9-C14 2.01(6), S1-C8-C9-C10 6.24(4), C13-C12-N3-C15 71.5(5), N3-C19-C20-C25 66.23(5), C16-C17-C26-C27 22.06(7).

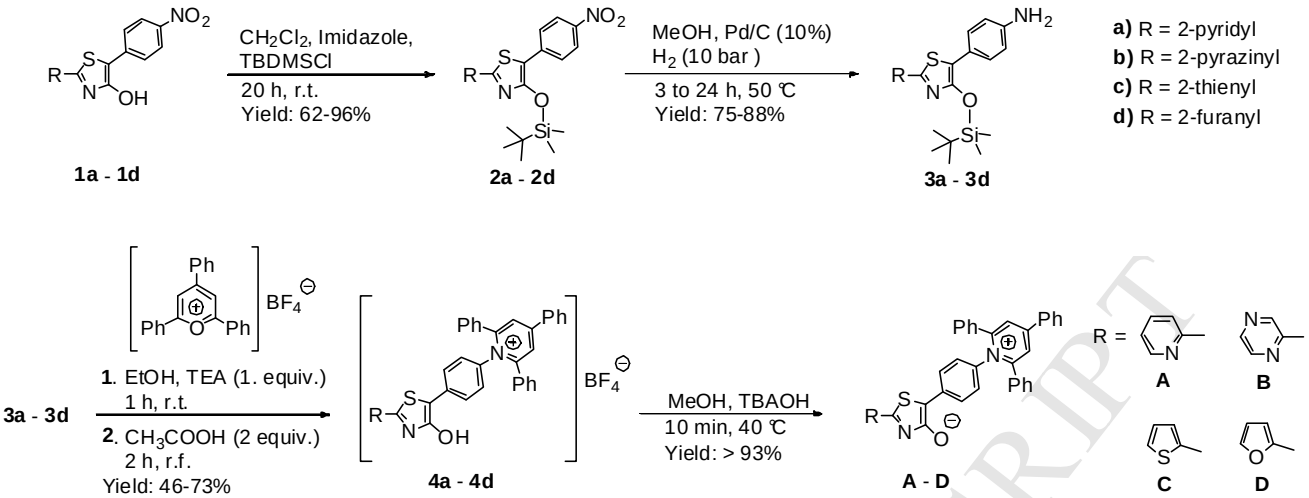

Scheme 1. Synthesis of the starting materials, cyclization reaction to the pyridinium salts and structures of the four betaine dyes **A-D**.

As expected, the thiophen-thiazole-phenyl moiety is almost completely planar [*e.g.* C7-C8-C9-C14 2.01(6) °] because of the change in the electron distribution. The zwitterionic structure leads to shortening of the single bonds, while the double bonds are elongated in this fragment. The bond of the deprotonated oxygen O1 to C7 of the thiazole becomes a double bond and, therefore, is significantly shortened [O1-C7 1.278(8) Å, compared to C-O saturated 1.43 Å, C=O in ketones 1.22 Å and C=O in zwitterion forms 1.26 Å][30] while the adjacent bonds are elongated [N2-C7 1.428(10) Å compared to N2-C7 1.369(7) Å for **4a**]. This is consistent with the partial quinoid character of the thiazol-4-olate ring. Also the bond between the thiazole-phenyl is shortened [C8-C9 1.405(9) Å compared to C8-C9 1.460(8) Å for **4a**] because of a partly double bond character in this position leading to the planarization observed. The thiophene moiety is displaced but both isomeric forms are planar with respect to the thiazole (torsion angle < 5 °). Therefore, it can be stated that deprotonation of the hydroxy group to the corresponding betaines significantly alters the geometry and the electronic properties. The bond lengths measured are in accordance with literature examples.[29]

2.3. Electronic Properties and Solvatochromism of the betaines

The color of a solution of the tetrafluoroborates **4a-4d** in MeOH changes from yellow to purple or almost black after deprotonation with TBAOH in MeOH and the betaines precipitated as purple to deep green solids (ESI S2). In order to gain insight into the electronic properties of the betaines **A-D**, firstly UV/Vis measurements were carried out in CH_3CN, a solvent with intermediate polarity and hydrogen bond donor (HBD) and hydrogen bond acceptor (HBA) character.[31] All of the dyes show several absorption bands of different intensities. The spectra together with the excited states calculated are shown in Figure 4. The spectra feature two main absorption bands. The absorption band of the excitations at 300 nm are independent of the solvent and are attributed to excitations of the 2,4,6-triarylpyridinium moiety (the band is also independent of the aryl-1,3-thiazole used).[32] As can be seen from the spectra, the longest wavelength absorption band at 470-670 nm, along with a red-sided shoulder, results from a superposition of at least two excited states. Both absorption bands are prone to differences of solvent properties and

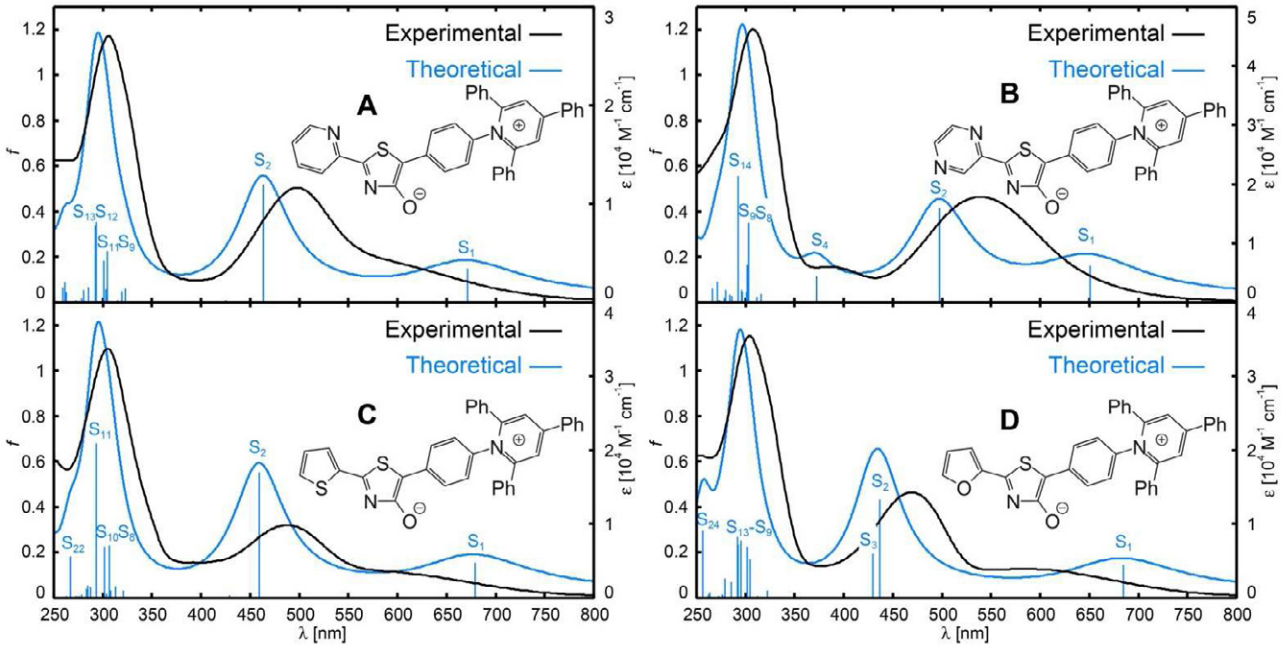

Figure 4. Experimental and simulated UV/Vis spectra of **A-D** at B3LYP(35)/6-31G(d,p) level of theory in CH_3CN at r.t. The calculated excited states were broadened using a full width of half maximum of 3000 cm^{-1}.

show a negative solvatochromism. The more intense absorption maximum is positioned at λ_{max} = 470 (**D**) to 540 nm (**B**) and is attributed to an excitation located at the heterocycle-1,3-thiazole-phenyl fragment. The band exhibits a less pronounced negative solvatochromic behavior, as can be seen from Table 1, compared to the excitation at the red-sided shoulder. The λ_{max} is shifted bathochromically in CH_3CN for the dyes with the pyridine or pyrimidine group in the 2-position, representing an electron-acceptor group, (partially CT-character of the transition) compared to the dyes bearing the furanyl or thienyl moiety (more π-π*-character). This is consistent with the electronic properties of the latter two, which contrarily possess more electron-donating properties. This absorption band was also found for similar donor-π-acceptor (D-π-A) dyes based on 4-methoxy-1,3-thiazoles.[23] A methoxy group was connected to the thiazole in the 4-position in the literature examples which represents a weaker electron-donor than the deprotonated hydroxy group and, consequently, the negative solvatochromism for this band was similar, but not as pronounced compared to the dyes presented here. The lower energy absorption band (shoulder at the red-side) is the most solvatochromic one and can be attributed to the intramolecular charge transfer (ICT) state typical for Reichardt's-type betaines (see section 2.4 for a more detailed description and Figure 5 for the correlated molecular orbitals).[5] The position of the band is strongly affected by the heterocycle in the 2-position. The absorption maximum in CH_3CN varies from 559 nm (**A**) to 613 nm (**C**) and is superimposed for **B** with the absorption of the higher energetic π-π*-CT state. It can be assumed that the bathochromic shift of the longest-wavelength absorption band for **C** and **D** is due to a partial participation of the electron donating thiophene and furan ring increasing the energy of the HOMO to efficiently enhance the ICT to the pyridinium group.

To get further insight into the solvatochromism of **A**-**D**, measurements in solvents with different polarities and different HBD (alcohols),[33] HBA (acetone, CH_3CN, DMSO, DMF) or non-HB properties (DCM, 1,2-dichloroethane) were carried out.[34] The polarity scale ranges from 1,1,1,3,3,3-hexafluoro-2-propanol (HFIP) [E_T(**30**) 65.3] to THF [E_T(**30**) 37.4]. The most polar solvent used, HFIP, did not yield reproducible results because of the high acidity (pK_a = 9.3),[35] which protonates the betaines at least to a certain extent. The spectra measured were almost identical to the spectra obtained from the BF_4^- salts in HFIP. Unfortunately, the compounds are insoluble in more unpolar solvents like heptane, toluene or cyclohexane excluding a better understanding of the solvatochromic behavior in these solvents. Although that in some solvents the two possible π-π* and ICT bands are superimposed, a clear trend of a pronounced negative solvatochromism was found. It was possible to simulate and resolve almost all the superimposed bands in an appropriate manner to obtain the λ_{max} of absorption by using the free available peak fitting program *Fityk*.[36] The solvatochromism determined is even more pronounced compared to the standard dye **30**. Compounds **C** and **D** exhibit the largest negative solvatochromism measured. This clearly follows the assumption made in the first part. For **C** and **D**, the additional electron donor in the 2-position (furanyl and thienyl) supports the electron rearrangement in the molecule from the negatively charged oxygen to the pyridinium part leading to a less dipolar S_1 state, which is extraordinarily well stabilized through unpolar solvent. This is contrary to **A** and **B**, where the additional electron acceptor in the 2-position leads to a S_1 state with a higher dipolar character and, therefore, a less pronounced negative solvatochromism. The regression parameters between the E_T(**X**) values of **A**-**D** and the E_T(**30**) were determined in order to get a more quantitative description of the solvatochromism. As expected, no good linear correlations were observed for any solvents. The HBD solvents (alcohols) especially do not follow the more or less linear trend of the other solvents, as depicted in the ESI S3. Two explanations can be found: (i) Contrary to **30**, no steric hindrance due to the two adjacent phenyl group exists in **A**-**D**, allowing hydrogen bond formation of R-OH to the thiazol-4-olate oxygen and (ii) additional hydrogen bond formation can be formed to the heterocycle in the 2-position (see also X-ray structure). Both cases stabilize the ground state to some extent and, consequently, make the ICT less accessible to changes in solvent polarity (*e.g.* changes of R in R-OH). This was also observed and described for similar dyes with pyridines (HBA) at the phenolic donor moiety.[3] Interactions of solutes with the solvent can be quite diverse. Therefore, Kamlet and Taft developed a more reasonable method to explain solvent properties. Intermolecular interactions of the solute/solvent system can be described by applying the concept of linear solvation energy relationships (LSERs, equation 1) using a multiple linear regression.[9,37,38]

$$\tilde{\nu}_{max} = \tilde{\nu}_{max,0} + a \times \alpha + b \times \beta + s \times \pi^* \qquad (1)$$

Table 1. Absorption maxima of the betaines **A**-**D** (both transitions are stated) and of the reference dye **30** together with their E_T(**X**) values in various solvents ordered according decreasing E_T(**30**) values at r.t. under normal pressure.

Solvent [a]	λ_{max} [nm] [E_T(**A**)] [b]	λ_{max} [nm] [E_T(**B**)] [b]	λ_{max} [nm] [E_T(**C**)] [b]	λ_{max} [nm] [E_T(**D**)] [b]	λ_{max} [nm] [E_T(**30**)] [b]
HFIP	369, 441 [64.8]	390, 460 [62.2]	393, 444 [64.4]	385, 455 [62.8]	438 [65.3]
TFE	373, 398 [71.8]	398, 474 [60.3]	376, 392 [72.9]	369, 403 [70.9]	478 [59.8]
MeOH	393, 446 [64.1]	400, 475 [60.2]	397, 434 [65.9]	413, 527 [54.3]	516 [55.4]
EtOH	388, 448 [63.8]	435, 485 [60.0]	453, 517 [55.3]	428, 553 [51.7]	551 [51.9]
n-Propanol	389, 451 [63.4]	439, 488 [58.6]	462, 522 [54.8]	426, 554 [51.6]	564 [50.7]
CH_3CN	493, 559 [51.1]	555 (sup.) [c]	483, 585 [48.9]	463, 613 [46.6]	627 [45.6]
DMSO	504, 593 [48.2]	560 (sup.) [c]	493, 600 [47.7]	472, 600 [47.7]	634 [45.1]
DMF	510, 580 [49.3]	560 (sup.) [c]	503, 624 [45.8]	497, 621 [46.0]	662 [43.2]
Acetone	500, 619 [46.2]	533, 592 [48.3]	495, 637 [44.9]	477, 635 [45.0]	678 [42.2}
NMP	525, 615 [46.5]	563, 630 [45.4]	510, 647 [44.2]	512, 645 [44.3]	678 [42.2]
Benzonitrile	489, 597 [47.9]	522, 575 [49.7]	488, 635 [45.0]	465, 627 [45.6]	689 [41.5]
1,2-Dichloroethane	462, 590 [48.5]	485, 560 [51.1]	460, 605 [47.3]	446, 593 [48.2]	692 [41.3]
DCM	492, 655 [43.7]	504, 637 [44.9]	440, 692 [41.3]	481, 675 [42.4]	702 [40.7]
Pyridine	526, 700 [40.8]	540, 653 [43.8]	522, 722 [39.6]	501, 720 [39.7]	706 [40.5]
$CHCl_3$	497, 734 [39.0]	514, 701 [40.8]	481, 759 [37.7]	482, 756 [37.8]	731 [39.1]
EtOAc	530, 715 [40.0]	541, 693 [41.3]	489, 724 [39.5]	495, 751 [38.1]	750 [38.1]
THF	540, 730 [39.2]	554, 730 [39.2]	526, 820 [34.9]	520, 823 [34.7]	764 [37.4]
	$\Delta\lambda$ = 332 [d]	$\Delta\lambda$ = 256 [d]	$\Delta\lambda$ = 428 [d]	$\Delta\lambda$ = 420 [d]	$\Delta\lambda$ = 286 [d]

[a] HFIP = 1,1,1,3,3,3-Hexafluoro-2-propanol, TFE = 2,2,2-Trifluoroethanol, DCM = Dichloromethane, [b] E_T(**X**) [kcal mol^{-1}] = hcN_A/λ_{max} = 28591/λ_{max} [nm], [c] superimposed, assignment would be tentative, [d] from THF to TFE in nm.

Here, the Kamlet-Taft parameters are as follows: α is the HBD acidity, β is the HBA basicity and π^* describes the dipolarity/polarizability of the solvent. Derived from the constants *a*, *b* and *s*, one can selectively determine the influence of either the HBD or HBA strength or the polarity of the solvent to the energy needed for excitation. Though there may be some controversies connected with the simplified Kamlet-Taft equation, it is still one of the easiest and best approaches to describe solvent effects and details can be found elsewhere.[9,39-41] The results of the multiple linear regressions can be found in Table 2. HFIP was again excluded and the parameters used can be found in the literature.[9]

Table 2. Regression coefficients *a*, *b* and *s* obtained for different multiple linear regressions of the Kamlet–Taft equation 1 for 16 solvents (13 for **B**) with correlation coefficient (*r*) and standard deviation (δ).

Comp.	$\tilde{\nu}_{max,0}$ [10^3 cm^{-1}] [a]	*a*	*b*	*s*	*r*	δ
A	8.027	8.065	3.450	7.347	**0.966**	1.021
	19.67	-	2.679	-4.588	0.305	3.635
	10.20	7.907	-	6.652	0.927	1.427
	14.00	6.817	3.095	-	0.924	1.461
B	8.862	5.286	3.345	7.135	**0.925**	1.199
C	6.128	8.403	1.780	9.712	**0.967**	1.007
D	5.743	7.066	0.579	10.94	**0.966**	0.850

[a] $\tilde{\nu}_{max,0}$ corresponds to the absorption maximum [cm^{-1}] in reference system cyclohexane (α, β and $\pi^* = 0$ by definition).

First of all, the relevant regressions obtained all show a very good correlation coefficient of ≥ 0.925. The regression coefficients are positive, indicating a negative, hypsochromic solvatochromism with increasing solvent dipolarity/polarizability and HBD or HBA strength. This is in accordance with the assumption that the S_0 state is more stabilized as a result of solvation with polar HBD molecules than the S_1 state. In all calculations using all three coefficients, *b* has the smallest influence, which is reasonable due to a missing HBD group in the betaines. Consequently, the regression excluding *b*, as exemplified for **A**, also yielded a very good *r* of 0.927, contrary to a multiple regression only using *b* and *s* as solvent parameters which yielded an unfeasible *r* of 0.305. In summary, the solvatochromic behavior of the betaines **A-D** is basically only influenced by the HBD acidity leading to interactions with the thiazol-4-olate (and minor with the heteroatom of the heterocycle in the 2-position) and from the polarity/polarizability of the solvent.

Additionally, the alternative solvent scales *SP*, *SdP*, *SB* and *SA*[42-45] from Catalán et al. with the mathematical expression shown in equation 2 were studied. They are considered to be slightly more precise than the Kamlet-Taft parameters when describing multiple solute-solvent interactions (especially in the differentiation between solvent dipolarity and polarizability), but generally yield very similar results.

$$\tilde{\nu}_{max} = \tilde{\nu}_{max,0} + a \times SA + b \times SB + c \times SP + d \times SdP \qquad (2)$$

In this multiple regression, *SA* corresponds to the acidity, *SB* to the basicity, *SP* to the polarizability and *SdP* to the dipolarity of the solvent and the values used can be found in the original publication from Catalán et. al.[45] The results of the multiple linear regressions are summarized in Table 3. The coefficients obtained are in accordance with the ones from the Kamlet–Taft equitation. The correlation coefficients for all important calculated regressions are > 0.884. The positive coefficients *a* and *d* (expressing *SA* and *SdP*) show the highest contributions, indicating a negative solvatochromism with higher HBD acidity and dipolarity of the solvent.

Table 3. Regression coefficients *a*, *b*, *c* and *d* obtained for different multiple linear regressions of the Catalán equation 2 for 16 solvents (13 for **B**) with correlation coefficient (*r*) and standard deviation (δ).

	$\tilde{\nu}_{max,0}$ [10^3 cm^{-1}] [a]	*a*	*b*	*c*	*d*	*r*	δ
A	12.70	10.96	1.249	-3.375	5.992	**0.944**	1.365
	27.76	-	-0.628	-24.89	9.597	0.751	2.623
	13.51	10.58	-	4.219	6.515	0.940	1.350
	18.23	11.38	-	3.533	-	0.911	1.577
	10.44	11.58	-	-	6.396	0.937	1.332
B	8.645	7.717	-1.132	2.917	5.903	**0.884**	1.563
C	10.94	10.90	-0.589	-3.407	8.214	**0.980**	0.833
D	9.378	8.706	-1.635	-0.846	8.361	**0.955**	1.023

[a] $\tilde{\nu}_{max,0}$ corresponds to the absorption maximum [cm^{-1}] in gas phase.

The neglectable contribution of the HBA basicity expressed through *b* is also similar to the LSER using Kamlet-Taft parameters. Regressions without *SB* yielded only very slightly lower correlation coefficients *r* than with this parameter. A very poor *r* was obtained for all betaines (illustrated for **A**) if the HBD acidity of the solvent was excluded from the regression. The main difference was observed by the differentiation between the polarizability and the dipolarity of the solvent. While an increasing polarizability *SP* causes a bathochromic shift (negative value for *c*), an increasing dipolarity *SdP* causes a hypsochromic shift (positive value for *d*). Nonetheless, the overall shift of the absorption maximum is hypsochromic in more polar solvents due to a higher contribution of *SdP* in all relevant regressions. This is also consistent with the dipolar nature of the betaines. It is worth mentioning that the intensity of the longest wavelength absorption diminished when solvent polarity decreased, similar to betaines presented in the literature,[13,46] This would be the main obstacle for an application of **A-D** as solvent polarity indicators.

2.4. Quantum Chemical Calculations on A-D

Density functional theory (DFT) and its time-dependent variant (TDDFT)[47] were applied in order to gain a deeper insight into the electronic and structural properties of the dyes. All calculations were performed with the GAUSSIAN 09 program.[48] The effects of solvation (CH_3CN, $\varepsilon = 35.688$, $n = 1.344$) were addressed with a polarized continuum model.[31] The ground state equilibrium structures of **A-D** were optimized using a functional based on B3LYP[49,50] and denoted as B3LYP(35),[51] combining 35% of exact-exchange, 58.5% of non-local B88[52] exchange, and the LYP correlation along with the 6-31G(d,p) double-ζ basis set.[53] Subsequent analyses of the harmonic vibrational frequency confirmed that the four stationary points of **A-D** correspond to minima of the respective potential energy surfaces. Excited state properties, such as excitation energies, oscillator strengths and excited state wavefunctions, were computed at the TDDFT level of theory with the same exchange correlation functional and basis set as the ground states. This functional allows a reasonable description of 4-hydroxy-thiazole based dyes as confirmed previously.[23] The absorption spectra of the four dyes were simulated from the first 30 singlet excited states.

The ground state equilibrium geometries of **A-D** show similar structural features. The phenyl moieties at the pyridinium ring are twisted out of planarity, while the torsion of the phenyl rings in the *ortho*-position is significantly enhanced (57 to 62°) contrary to the phenyl ring in the *para*-position (33°). Additionally, the *N*-phenyl ring is twisted by approximately 70° due to steric reasons. The remaining 1,3-thiazol-4-olate fragment is completely planar, contrary to the X-ray structure of **4a** presented in Figure 2 or 4-methoxy-1,3-thiazole-based dyes previously studied.[20] Naturally, the reason is the zwitterionic structure of the dyes confirmed by the bond length alternation (BLA) indices,[54,55] defined as the difference between the average C-C and C=C bond lengths of -0.0239 Å, -0.0211 Å, -0.0128 Å, and -0.0118 Å for the dyes **A** to **D**. Hence, single bonds are shortened, while double bonds are stretched. This effect is illustrated for the C-O bonds with bond

lengths of approximately 1.25 Å consistently with the solid state structure of **C**. The dipolar ionic structure was also confirmed by natural bond orbital (NBO) analysis and the corresponding electrostatic potentials of the dyes (for representations, see ESI S4-S7).

A Lorentzian function with a full width of half maximum of 3000 cm^{-1} was employed to broaden the transitions based on the calculated oscillator strengths of the first 30 singlet excited states. The absorption spectra of the dyes feature an intense band in the visible region at approximately 470-540 nm together with a less intense band at 550-620 nm, while the UV region shows a very intense band at approximately 300 nm. Furthermore, **B** exhibit a minor band located at 387 nm. The composition of the transitions in the visible range are revealed in Table 4 and the molecular orbitals (MOs) are shown in Figure 5, while a summary of the predominant excited states in the UV region is provided in ESI S8 and respective MOs are shown in ESI S9. The absolute energies of the MOs depicted in Figure 5 are additionally given in ESI 10. The lowest energy band is determined by the S_1 states and was found to be an ICT state from the HOMO located at the thiazol-4-olate-phenyl fragment to the LUMO located at the pyridinium moiety (see Figure 5). Oscillator strengths (*f*) from 0.145 to 0.162 point to medium strength absorbing states. The excitation energy for **C** and **D** was calculated to 1.81 and 1.82 eV and increases to 1.85 and further to 1.90 eV for **A** and **B**, respectively. On the other hand, the second more intense absorption bands in the Vis region of **A** and **B** result from less pronounced ICT states (S_2) from the HOMOs to the LUMO+1 orbitals. The latter are mainly centered at the thiazole and the pyridine/pyrazine rings. Substitution of the pyridine moiety (**A**) with pyrazinyl (**B**) decreases the excitation energy from 2.68 to 2.49 eV, while *f* is also decreased from 0.520 to 0.414. The excited state wavefunctions of the S_2 states of **C** and **D** (see Table 4) feature a pronounced mixing of a transition from the HOMO to the 1,3-thiazole-thienyl/furanyl fragment (LUMO+1/LUMO+2) and a transition from the HOMO to the pyridinium ring (LUMO+2/LUMO+1). This mixing is accompanied by an increase of the S_2 excitation energy to 2.70 and 2.84 eV, while the oscillator strength decreases with the mixing ratio of these transitions from 0.553 to 0.432. In the case of **D**, a further medium strength (0.1971) ICT state (S_3) of inverted mixing ratio was found at 2.89 eV. In fact, this state is correlated to the shoulder at the higher energetic side of the band at 460 nm. In summary, the results of the quantum chemical calculations correlate very well with experimental data and allowed an unambiguous assignment of the electronic states to the absorption bands. The excitation energies obtained of the S_1 are underestimated by -0.21 to -0.37 eV, while the energies of the S_2 are overestimated by 0.13 to 0.21 eV. For reasons of comparison, the excited states of **A** have also been studied using the long-range corrected CAM-B3LYP functional; however, the deviations from the experiment were significantly increased and results are not shown here.

Table 4. Calculated excitations of **A**-**D** of the singlet excited states in CH_3CN in the visible region. Main contributions to the wavefunction (weight), vertical excitation energies (ΔE^e) oscillator strengths (*f*) and deviations from experimental peak values ($\Delta\Delta E_{Exp}$).

State	Transition	Weight [%]	ΔE^e [eV]	[nm]	*f*	$\Delta\Delta E_{exp}$ [eV]
		A				
S_1	HOMO→LUMO	99	1.85	672	0.149	-0.37
S_2	HOMO→LUMO+1	96	2.68	463	0.520	+0.17
		B				
S_1	HOMO→LUMO	98	1.90	651	0.162	-
S_2	HOMO→LUMO+1	99	2.49	497	0.414	+0.19
		C				
S_1	HOMO→LUMO	98	1.82	679	0.156	-0.30
S_2	HOMO→LUMO+1	81	2.70	459	0.553	+0.13
	HOMO→LUMO+2	18				
		D				
S_1	HOMO→LUMO	99	1.81	685	0.145	-0.21
S_2	HOMO→LUMO+2	60	2.84	437	0.432	+0.16
	HOMO→LUMO+1	38				
S_3	HOMO→LUMO+1	60	2.89	429	0.197	+0.21
	HOMO→LUMO+2	39				

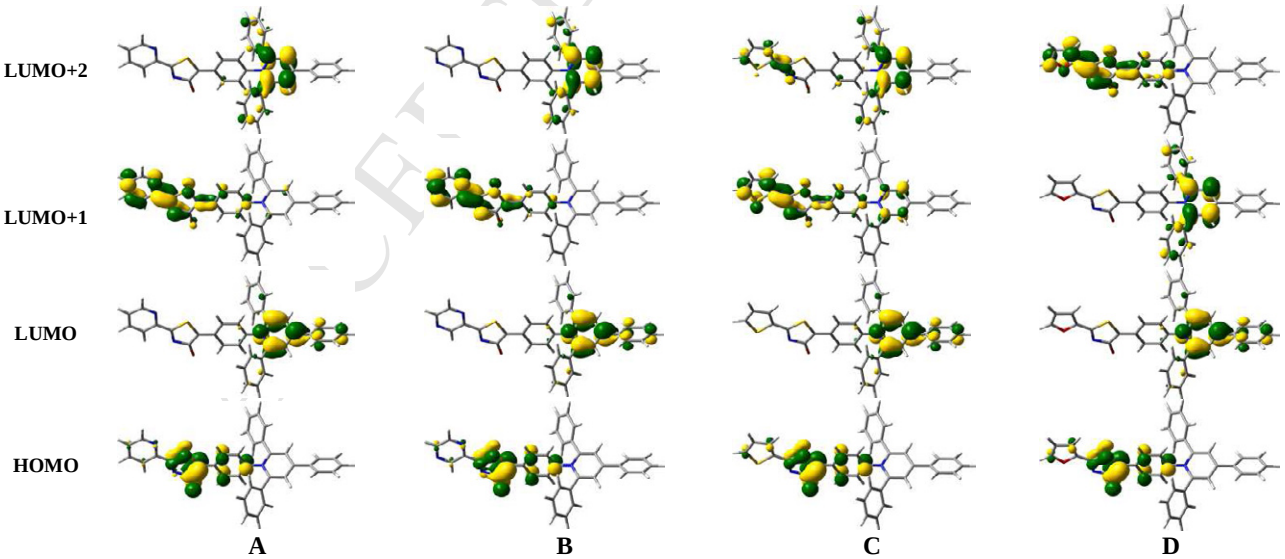

Figure 5. Molecular orbitals involved in the main singlet excited states of the dyes **A**-**D** at B3LYP(35)/6-31G(d,p) level of theory in CH_3CN contributing to the absorption in the visual region.

3. Conclusion

This paper presents the synthesis and thorough characterization concerning the optical properties of unusual Reichardt's-type betaines. The commonly used phenolic donor group was substituted by a thiazol-4-olate which acts as donor as well as chromophoric unit. The possible different transitions were unambiguously assigned and described using spectroscopic, multiparametric correlation (LSER) and quantum chemical methods. The longest wavelength absorption band is of intense ICT character and prone mainly to changes in HBD acidity and polarity of the solvents. Compound **D** proved to be best qualified to meassure changes in solvent properties while compound **A** and **B** are less suited due to a more pronounced superimposition of the $S_0 \rightarrow S_1$ and $S_0 \rightarrow S_2$ transition. For further research the focus will be placed on the synthesis of dyes with a (hetero)aryl in the 4-position of the thiazole bearing stronger electron donor groups to influence the ICT (to obtain better resolved absorption bands) and/or different moieties (alkyl chains, fluorinated chains, sulfonates) to obtain a distinct solubility. Also the connections with other heterocycles (*e.g.* pyrrole) increasing possible interactions with solvent molecules and influencing the optical properties will be considered. Finally, interactions with molecules mimicking nucleic bases pairs to obtain sensor molecules for molecular recognition, as shown from Bolz *et al*.,[13] will be the subject of subsequent studies.

4. Experimental section

4.1. General

5-(4-Nitrophenyl)-2-(pyridin-2-yl)thiazol-4-ol (**1a**) 5-(4-nitrophenyl)-2-(pyrazin-2-yl)thiazol-4-ol (**1b**), 5-(4-nitrophenyl)-2-(thiophen-2-yl)thiazol-4-ol (**1c**) and ethyl 2-bromo-2-(4-nitrophenyl)acetate were synthesized according to literature procedures.[23,20,56] Furan-2-carbothioamide is commercially available or can be prepared from the corresponding nitrile and H_2S in EtOH in the presence of Et_3N.[57] All other chemicals used were reagent grade and purchased from Sigma-Aldrich or Alfa Aesar. Solvents were purified according to standard procedures. Solvents for UV/Vis were of analytical grade and purchased from Sigma-Aldrich. ^{1}H-, ^{13}C-NMR and the corresponding correlation spectra were recorded on a Bruker AC-250 (250 MHz) and AC-400 (400 MHz) spectrometer. Chemical shifts (δ) are given relative to solvents. UV/Vis data of the compounds were collected on a Lambda 19 from PERKIN-ELMER. Elemental analysis was carried out on a Leco CHNS-932. Mass spectra were measured either on a Finnigan MAT SSQ 710 (EI) or MAZ 95 XL (FAB) system. MALDI TOF MS was performed on a Bruker Ultraflex TOF/TOF mass spectrometer equipped with a 337 nm nitrogen laser operated in the reflectron mode using an acceleration voltage of 25 kV, and dithranol (Bruker, #209783) was used as matrix. TLC was from Merck (Polygram SIL G/UV254, aluminum oxide 60 F254). The material for Column chromatography was also obtained from Merck (Silica gel 60).

X-Ray: The intensity data for the compounds were collected on a Nonius KappaCCD diffractometer using graphite-monochromated Mo-K_α radiation. Data were corrected for Lorentz and polarization effects but not for absorption effects.[58,59] The structure was solved by direct methods (SHELXS) and refined by full-matrix least squares techniques against Fo^2 (SHELXL-97).[60] All hydrogen atoms were included at calculated positions with fixed thermal parameters. All non-hydrogen atoms were refined anisotropically.[60] XP (SIEMENS Analytical X-ray Instruments, Inc.) was used for structure representations.

4.2. General procedure for the preparation of the 4-hydroxy-1,3-thiazoles

A suspension of the thioamide (10 mmol) and ethyl 2-bromo-2-(4-nitrophenyl)acetate (13 mmol, 1.3 equiv.) in toluene (20 mL) under a nitrogen atmosphere were heated under reflux conditions for 4 h. An orange solid precipitated. Pyridine was added to the hot solution and the mixture was further stirred for additional 4 h while cooling down to r.t. The solid was filtered off and washed with EtOH and pentane. The pure compounds were obtained as crystalline solids after recrystallization from EtOH/DMF.

*4.2.1. 2-(Furan-2-yl)-5-(4-nitrophenyl)thiazol-4-ol (**1d**).* Brown crystals (1.70 g, 59%). MP >330 °C decompose. ^{1}H NMR (250 MHz, DMSO-d_6): δ = 12.59 (s, 1H), 8.23 (d, *J* 9.0 Hz, 2H), 7.98-7.86 (m, 3H), 7.12 (d, *J* 3.5 Hz, 1H), 6.75 (dd, *J* 3.5, 1.8 Hz, 1H). ^{13}C NMR (63 MHz, DMSO-d_6): δ = 161.14, 152.60, 147.74, 145.68, 144.24, 138.88, 125.75, 124.28, 113.08, 110.45, 104.69. MS (EI): *m/z* (%) 288 (100) [M^+]. Anal. Calcd for $C_{13}H_8N_2O_4S$: C, 54.16; H, 2.80; N, 9.72; S, 11.12. Found: C, 53.19; H, 2.80; N, 9.73; S, 11.24.

4.3. General procedure for the preparation of the silylethers

To a suspension of the corresponding 4-hydroxy-1,3-thiazole (10 mmol) and imidazole (20 mmol) in CH_2Cl_2 (100 mL, dry) was added *tert*-butyldimethylsilyl chloride (12 mmol). The solution was stirred under a nitrogen atmosphere for 24 h, washed with H_2O (3×50 mL), dried over $MgSO_4$ and concentrated till dryness *in vacuo*. The silyl ethers were purified using column chromatography (silica, $CHCl_3$) or by recrystallization from EtOH/CH_2Cl_2 by slowly evaporating of the latter, yielding the compounds as yellow to orange-brown crystalline solids.

*4.3.1. 4-((tert-Butyldimethylsilyl)oxy)-5-(4-nitrophenyl)-2-(pyridin-2-yl)thiazole (**2a**).* Yellow fluffy crystalline solid (3.56 g, 85%). MP 224.0-224.4 °C. ^{1}H NMR (300 MHz, $CDCl_3$): δ = 8.60 (d, *J* 4.7 Hz, 1H), 8.21 (d, *J* 9.0 Hz, 2H), 8.05 (d, *J* 7.9 Hz, 1H), 7.93 (d, *J* 9.0 Hz, 2H), 7.80 (td, *J* 7.8, 1.6 Hz, 1H), 7.33 (ddd, *J* 7.4, 4.6, 0.9 Hz, 1H), 1.06 (s, 9H), 0.44 (s, 6H). ^{13}C NMR (75 MHz, $CDCl_3$): δ 162.90, 158.28, 150.62, 149.54, 145.43, 139.00, 137.03, 126.56, 124.79, 124.02, 119.23, 113.12, 25.90, 18.15, -3.98. MS (EI): *m/z* (%) 413 (15) [M^+], 356 (100). Anal. Calcd for $C_{20}H_{23}N_3O_3SSi$: C, 58.08; H, 5.61; N, 10.16; S, 7.75. Found: C, 58.17; H, 5.78; N, 10.21; S 7.33. UV/Vis (CH_2Cl_2): λ_{max} (log ε): 223 (4.22), 275 (4.07), 394 (4.39).

*4.3.2. 4-((tert-Butyldimethylsilyl)oxy)-5-(4-nitrophenyl)-2-(pyrazin-2-yl)thiazole (**2b**).* Yellow orange solid (4.00 g, 96%). MP 190.0 °C. ^{1}H NMR (250 MHz, $CDCl_3$): δ = 9.31 (d, *J* 1.5 Hz), 8.61 (d, *J* 2.5 Hz), 8.56 (dd, *J* 2.5, 1.5 Hz), 8.31-8.18 (m), 8.03-7.90 (m), 1.07 (s), 0.45 (s).^{13}C NMR (63 MHz, $CDCl_3$): δ = 159.87, 158.60, 146.16, 145.81, 145.32, 143.98, 141.12, 138.46, 126.85, 124.10, 114.35, 25.89, 18.19, -3.98. MS (EI): *m/z* (%) 414 (15) [M^+], 357 (100). Anal. Calcd for $C_{19}H_{22}N_4O_3SSi$: C, 55.05; H, 5.35; N, 13.51; S, 7.73. Found: C, 54.96; H, 5.05; N, 13.30; S, 7.46.

*4.3.3. 4-((tert-Butyldimethylsilyl)oxy)-5-(4-nitrophenyl)-2-(thiophen-2-yl)thiazole (**2c**).* Orange crystalline solid (3.01 g, 72%). MP 185.0-185.3 °C. ^{1}H NMR (250 MHz, $CDCl_3$): δ = 8.26-8.16 (m, 2H), 7.90-7.82 (m, 2H), 7.52 (dd, *J* = 3.7 Hz, 1.0 Hz, 1H), 7.42 (dd, *J* = 5.0 Hz, 1.0 Hz, 1H), 7.10 (dd, *J* = 5.0 Hz, 3.8 Hz, 1H), 1.06 (s, 9H), 0.42 (s, 6H). ^{13}C NMR (63 MHz, $CDCl_3$): δ = 157.96, 156.53, 145.31, 139.09, 137.56, 128.72, 128.31, 126.56, 126.31, 124.25, 109.40, 26.11, 18.34,

-3.86. MS (EI): *m/z* (%) 418 (20) [M^+], 361 (100). Anal. Calcd for $C_{19}H_{22}N_2O_3S_2Si$: C, 54.52; H, 5.30; N, 6.69; S, 15.32. Found: C, 54.32; H, 5.33; N, 7.01; S, 15.58.

*4.3.4. 4-((tert-Butyldimethylsilyl)oxy)-2-(furan-2-yl)-5-(4-nitrophenyl)thiazole (**2d**).* Brown thick needles (2.50 g, 62%). MP 166.0-166.3 °C. ^{1}H NMR (250 MHz, $CDCl_3$): δ = 8.26-8.15 (m, 2H), 7.95-7.81 (m, 2H), 7.52 (d, *J* 1.5 Hz, 1H), 6.98 (d, *J* 3.5 Hz, 1H), 6.56 (dd, *J* 3.4, 1.7 Hz, 1H), 1.05 (s, 9H), 0.40 (s, 6H). ^{13}C NMR (63 MHz, $CDCl_3$): δ = 158.47, 152.51, 149.11, 145.36, 144.22, 139.14, 126.37, 124.24, 112.67, 109.75, 109.69, 26.09, 18.32, -3.87. MS (EI): *m/z* (%) 402 (50) [M^+], 345 (100). Anal. Calcd for $C_{19}H_{22}N_2O_4SSi$: C, 56.69; H, 5.51; N, 6.96; S, 7.97. Found: C, 56.71; H, 5.49; N, 6.87; S, 7.66.

4.4. General procedure for the reduction of the nitro group to the corresponding amines

The corresponding nitro compound (5.0 mmol) was dissolved in THF (50 mL) in an autoclave (Büchi AG, model: miniclave steel) and a spate Pd/C was added. Hydrogen was applied (max. 10 bar) under continuous stirring at r.t, or if the reaction proceeds slow, at slightly elevated temperature (max. 50 °C). After the reaction was finished (3-10 h) as indicated by TLC (silica, $CHCl_3$; the educts elute at the front, while the amines do not elute) the catalyst was filtered off and the remaining solution was concentrated *in vacuo*. A short gel filtration (silica, $CHCl_3$ to $CHCl_3$/EtOAc 2:1) yielded the amines as yellow solids or oils which solidify after a while.

*4.4.1. 4-(4-((tert-Butyldimethylsilyl)oxy)-2-(pyridin-2-yl)thiazol-5-yl)aniline (**3a**).* Yellow solid (1.59 g, 83%). MP 132.9-133.2 °C. ^{1}H NMR (250 MHz, $CDCl_3$): δ = 8.56 (d, *J* 4.8 Hz, 1H), 8.02 (d, *J* 7.9 Hz, 1H), 7.74 (td, *J* 7.8, 1.7 Hz, 1H), 7.61 (d, *J* 8.6 Hz, 2H), 7.22 (m, 1H), 6.70 (d, *J* 8.6 Hz, 2H), 3.74 (s, 2H), 1.04 (s, 9H), 0.37 (s, 6H). ^{13}C NMR (63 MHz, $CDCl_3$): δ = 157.97, 155.23, 151.74, 149.46, 145.46, 136.93, 128.35, 123.80, 122.56, 118.91, 116.71, 115.24, 77.16, 26.14, 18.35, -3.84. MS (EI): *m/z* (%) 383 (100) [M^+], 326 (90). Anal. Calcd for $C_{19}H_{22}N_2O_4SSi$: C, 62.62; H, 6.57; N, 10.95; S, 8.36. Found: C, 62.69; H, 6.89; N, 10.94; S 8.11.

*4.4.2. 4-(4-((tert-Butyldimethylsilyl)oxy)-2-(pyrazin-2-yl)thiazol-5-yl)aniline (**3b**).* Red orange solid (1.52 g, 79%). MP 155.0-155.2 °C. ^{1}H NMR (250 MHz, $CDCl_3$): δ = 9.27 (d, *J* 1.3 Hz, 1H), 8.50-8.45 (m, 2H), 7.64-7.57 (m, 2H), 6.73-6.66 (m, 2H), 3.77 (s, 2H), 1.04 (s, 9H), 0.38 (s, 6H). ^{13}C NMR (63 MHz, $CDCl_3$): δ = 155.66, 154.73, 147.11, 145.85, 144.09, 143.81, 140.99, 128.40, 121.88, 118.23, 115.13, 26.05, 18.28, -3.92. MS (EI): *m/z* (%) 384 (90) [M^+], 327 (100). Anal. Calcd for $C_{19}H_{24}N_4OSSi$: C, 59.34; H, 6.29; N, 14.57; S, 8.34. Found: C, 59.31; H, 6.29; N, 14.53; S, 8.17.

*4.4.3. 4-(4-((tert-Butyldimethylsilyl)oxy)-2-(thiophen-2-yl)thiazol-5-yl)aniline (**3c**).* Orange solid (1.75 g, 88%). MP 175.0-175.5 °C. ^{1}H NMR (250 MHz, $CDCl_3$): δ = 7.58-7.49 (m, 2H), 7.40 (dd, *J* = 3.7 Hz, 1.0 Hz, 1H), 7.31 (dd, *J* = 5.0 Hz, 0.9 Hz, 1H), 7.04 (dd, *J* = 5.0 Hz, 3.7 Hz, 1H), 6.73-6.65 (m, 2H), 1.03 (s, 9H), 0.36 (s, 6H). ^{13}C NMR (63 MHz, $CDCl_3$): δ = 154.29, 51.87, 145.16, 138.58, 128.06, 127.92, 126.89, 124.83, 122.43, 115.26, 112.47, 26.17, 18.35, -3.90. MS (EI): *m/z* (%): 388 (100) [M^+] 331 (95). Anal. Calcd for $C_{19}H_{24}N_2OS_2Si$: C, 58.72; H, 6.22; N, 7.21; S, 16.50. Found: C, 58.72; H, 5.95; N, 6.95; S 16.83.

*4.4.4. 4-(4-((tert-Butyldimethylsilyl)oxy)-2-(furan-2-yl)thiazol-5-yl)aniline (**3d**).* Yellow solid (1.40 g, 75%). MP 93.0-93.3 °C. ^{1}H NMR (400 MHz, $CDCl_3$): δ = 7.58-7.52 (m, 2H), 7.45 (dd, *J* 1.7, 0.6 Hz, 1H), 6.86 (dd, *J* 3.4, 0.6 Hz, 1H), 6.73-6.66 (m, 2H), 6.50 (dd, *J* 3.4, 1.8 Hz, 1H), 3.72 (s, 2H), 1.02 (s, *J* 2.8 Hz, 9H), 0.34 (s, *J* 3.2 Hz, 6H). ^{13}C NMR (100 MHz, $CDCl_3$): δ = 154.88, 149.81, 148.16, 145.18, 143.01, 128.14, 122.42, 115.26, 112.81, 112.26, 107.62, 26.13, 18.32, -3.91. MS (EI): *m/z* (%) 372 (70) [M^+], 315 (100). Anal. Calcd for $C_{19}H_{24}N_2O_2SSi$: C, 61.25; H, 6.49; N, 7.52; S, 8.61. Found: C, 61.45; H, 6.59; N, 7.36; S, 8.85.

4.5. General procedure for the preparation of the pyridinium tetrafluoroborate salts

To a suspension of the corresponding amine (2.0 mmol) and 2,4,6-triphenylpyrylium tetrafluoroborate (2.0 mmol) in EtOH (20 mL) in a round bottle flask was added Et_3N (2.0 mmol). The mixture turned deep brown while the educts dissolved and was stirred for 30 min at r.t. followed by the addition of AcOH (4.0 mmol) and heating under reflux conditions for additional 2 h. The product precipitated during the reaction. The product was dissolved directly in the flask with little acetone at the reflux temperature after the reaction was finished (no further precipitate occurred). After cooling down to r.t. the product crystallized as a yellow solid which was filtered off, washed with cold EtOH and pentane and dried *in vacuo*.

*4.5.1. 1-(4-(4-Hydroxy-2-(pyridin-2-yl)thiazol-5-yl)phenyl)-2,4,6-triphenylpyridin-1-ium tetrafluoroborate (**4a**).* Orange crystalline solid (0.93 g, 72%). MP >255 °C decompose. ^{1}H NMR (400 MHz, DMSO-d_6): δ = 8.65 (s, 2H), 8.60 (d, *J* = 4.7 Hz, 1H), 8.34 (d, *J* = 6.9 Hz, 2H), 8.00-7.91 (m, 2H), 7.74-7.64 (m, 3H), 7.57 (d, *J* = 8.7 Hz, 2H), 7.53-7.35 (m, 13H), 4.34 (s, 1H). ^{13}C NMR (100 MHz, DMSO-d_6): 161.89, 159.99, 156.44, 155.51, 149.75, 137.80, 136.49, 133.40, 133.07, 132.54, 130.03, 129.72, 129.08, 128.79, 128.19, 125.27, 125.19, 125.14, 118.64, 108.23. MS (EI): *m/z* (%) 559 (<1) [M-BF_4^-]$^+$, 426 (<1), 307 (100). Anal. Calcd for $C_{37}H_{26}BF_4N_3OS$: C, 67.54; H, 4.65; N, 6.06; S, 4.62. Found: C, 67.50; H, 4.72; N, 6.12; S, 4.56.

*4.5.2. 1-(4-(4-Hydroxy-2-(pyrazin-2-yl)thiazol-5-yl)phenyl)-2,4,6-triphenylpyridin-1-ium tetrafluoroborate (**4b**).* Yellow crystalline solid (0.95 g, 73%). MP >250 °C decompose. ^{1}H NMR (400 MHz, DMSO-d_6): ^{1}H NMR (400 MHz, DMSO-d_6): δ = 12.27 (s, 1H), 9.17 (d, *J* = 15.4 Hz, 1H), 8.81-8.60 (m, 4H), 8.37 (d, *J* = 7.1 Hz, 2H), 7.75-7.64 (m, 3H), 7.61 (d, *J* = 8.6 Hz, 2H), 7.56-7.45 (m, 6H), 7.45-7.32 (m, 6H). ^{13}C NMR (100 MHz, DMSO-d_6): 160.26, 159.05, 156.42, 155.52, 145.87, 145.26, 144.63, 139.87, 136.90, 133.42, 133.10, 132.91, 132.57, 130.05, 129.75, 129.20, 128.85, 128.23, 125.39, 125.19, 109.55. MS (EI): *m/z* (%) 561.1 (1) [M-BF_4^-]$^+$, 427 (1), 307 (100). $C_{36}H_{25}BF_4N_4OS$: C, 66.68; H, 3.89; N, 8.64; S, 4.94. Found: C, 66.96; H, 3.90; N, 8.77; S, 4.55.

*4.5.3. 1-(4-(4-Hydroxy-2-(thiophen-2-yl)thiazol-5-yl)phenyl)-2,4,6-triphenylpyridin-1-ium tetrafluoroborate (**4c**).* Yellow-orange solid (0.60 g, 46%). MP 262.0-263.5 °C. ^{1}H NMR (400 MHz, DMSO-d_6): δ = 12.06 (s, 1H), 8.66 (s, 2H), 8.36 (d, *J* = 8.0 Hz, 2H), 7.74 (dd, *J* = 5.1 Hz, 1.0 Hz, 1H), 7.72-7.63 (m, 3H), 7.60 (dd, *J* = 3.7 Hz, 1.0 Hz, 1H), 7.55-7.30 (m, 14H), 7.17 (dd, *J* = 5.0 Hz, 3.8 Hz, 1H). ^{13}C NMR (100 MHz, DMSO-d_6): 159.06, 156.44, 155.48, 155.34, 136.27, 136.26, 133.42, 133.12, 133.08, 132.56, 130.03, 129.75, 129.50, 129.11, 128.84, 128.77, 128.20, 127.14, 125.18, 124.83, 104.64. MS (EI): *m/z* (%) 565 (1) [M-BF_4^-]$^+$, 427 (1), 307 (100). Anal. Calcd for $C_{36}H_{25}BF_4N_2OS_2$: C, 66.26; H, 3.86; N, 4.29; S, 9.83. Found: C, 66.30; H, 3.70; N, 4.21; S, 9.76.

*4.5.4. 1-(4-(2-(Furan-2-yl)-4-hydroxythiazol-5-yl)phenyl)-2,4,6-triphenylpyridin-1-ium tetrafluoroborate (**4d**).* Orange solid (0.88 mg, 63%). MP >230 °C decomp. ^{1}H NMR (400 MHz, DMSO-d_6): δ = 12.08 (s, 1H), 8.66 (s, 2H), 8.36 (d, *J* 7.4 Hz, 2H), 7.88 (s, 1H), 7.74-7.63 (m, 3H), 7.53-7.36 (m, 14H), 7.02 (d, *J* 2.9 Hz, 1H), 6.71 (s, 1H). ^{13}C NMR (100 MHz, DMSO-d_6): δ = 159.80, 156.44, 155.45, 151.01, 147.82, 145.22, 136.24, 133.41, 133.12, 132.53, 130.00, 129.72, 129.08, 128.82, 128.19, 125.17, 124.76, 112.94, 109.73, 104.57. MS (Micro-ESI): 549 $[M\text{-}BF_4^-]^+$. Anal. Calcd for $C_{36}H_{25}BF_4N_2O_2S$: C, 67.94; H, 3.96; N, 4.40; S, 5.04. Found: C, 67.85; H, 3.91; N, 4.44; S, 4.77.

4.6. General procedure for the preparation of the betaines

To a suspension of the corresponding tetrafluoroborate salt (1.0 mmol) in MeOH (15 mL) was added tetrabutylammonium hydroxide (1.1 mmol). The mixture was stirred for 1 h at 40 °C. The deep purple to black precipitate (Et_2O was added if the compound did not precipitate sufficiently) was filtered off after cooling down to r.t. and was washed with little EtOH and Et_2O and dried *in vacuo*.

*4.6.1. 2-(Pyridin-2-yl)-5-(4-(2,4,6-triphenylpyridin-1-ium-1-yl)phenyl)thiazol-4-olate (**A**).* Dark purple solid (543 mg, 97%). MP >245 °C decompose. ^{1}H NMR (400 MHz, DMSO-d_6): δ = 8.56 (s, 2H), 8.48 (d, *J* = 4.5 Hz, 1H), 8.31 (d, *J* = 6.8 Hz, 2H), 7.88 (d, *J* = 7.9 Hz, 1H), 7.80 (td, *J* = 7.8 Hz, 1.4 Hz, 1H), 7.73-7.58 (m, 5H), 7.53-7.44 (m, 4H), 7.42-7.34 (m, 6H), 7.30 (dd, *J* = 6.6 Hz, 5.5 Hz, 1H), 7.06 (d, *J* = 8.9 Hz, 2H). ^{13}C NMR (100 MHz, DMSO-d_6): 173.44, 158.63, 156.72, 154.76, 151.61, 149.17, 139.43, 136.96, 133.52, 133.49, 132.29, 131.25, 129.78, 129.65, 128.69, 128.11, 127.73, 125.18, 123.61, 121.30, 118.63, 109.46, 97.44. MS (MALDI-TOF, dithranol): *m/z* 560.32 for $C_{37}H_{26}N_3OS$ ($[M + H]^+$). Requires: 560.18. Anal. Calcd for $C_{37}H_{25}N_3OS$: C, 79.40; H, 4.50; N, 7.51; S, 5.73. Found: C, 79.23; H, 4.53; N, 7.39; S, 5.67.

*4.6.2. 2-(Pyrazin-2-yl)-5-(4-(2,4,6-triphenylpyridin-1-ium-1-yl)phenyl)thiazol-4-olate (**B**).* Dark purple solid (549 mg, 98%). MP 235 °C. ^{1}H NMR (250 MHz, DMSO-d_6) δ = 9.04 (s, 1H), 8.55 (d, *J* = 16.9 Hz, 4H), 8.32 (d, *J* = 6.3 Hz, 2H), 7.74-7.58 (m, 5H), 7.56-7.30 (m, 10H), 7.08 (d, *J* = 8.9 Hz, 2H). ^{13}C NMR (63 MHz, DMSO-d_6): δ = 156.69, 155.38, 154.75, 146.90, 144.16, 143.92, 140.22, 139.18, 133.50, 132.30, 131.57, 129.77, 129.66, 128.73, 128.11, 127.79, 125.16, 121.39, 98.13. MS (ESI): 561.2 $[M + H]^+$. MS (MALDI-TOF, dithranol): *m/z* 561.31 for $C_{36}H_{25}N_4OS$ ($[M + H]^+$). Requires: 561.17.

*4.6.3. 2-(Thiophen-2-yl)-5-(4-(2,4,6-triphenylpyridin-1-ium-1-yl)phenyl)thiazol-4-olate (**C**).* Dark deep-brown fluffy solid (530 mg, 94%). >217 °C decomp. Column Chromatography possible (silica, MeOH, R_f = 0.6). ^{1}H NMR (400 MHz, MeOD-d_4): δ = 8.48 (s, *J* = 6.0 Hz, 2H), 8.15 (dd, *J* = 7.7 Hz, 1.8 Hz, 2H), 7.71-7.65 (m, 3H), 7.60 (d, *J* = 8.7 Hz, 2H), 7.51-7.43 (m, 6H), 7.43-7.32 (m, 6H), 7.12 (d, *J* = 8.8 Hz, 2H), 7.07 (dd, *J* = 5.0 Hz, 3.8 Hz, 1H). ^{13}C NMR (100 MHz, DMSO-d_6): 156.69, 154.60, 152.09, 139.52, 139.36, 133.57, 133.52, 132.27, 130.52, 129.71, 129.67, 129.63, 128.70, 128.18, 128.08, 128.02, 127.96, 127.68, 126.96, 125.14, 124.06, 120.64, 92.61.MS (MALDI-TOF, dithranol): *m/z* 565.28 for $C_{36}H_{25}N_2OS_2$ ($[M + H]^+$). Requires: 560.14. Calcd for $C_{36}H_{24}N_2OS_2$: C, 76.57; H, 4.28; N, 4.96; S, 11.36. Found: C, 76.51; H, 4.01; N, 5.66; S, 11.03.

*4.6.4. 2-(Furan-2-yl)-5-(4-(2,4,6-triphenylpyridin-1-ium-1-yl)phenyl)thiazol-4-olate (**D**).* Dark green solid (512 mg, 93%). MP >250 °C decomp. ^{1}H NMR (100 MHz, DMSO-d_6) δ = 8.58 (s, 2H), 8.35-8.29 (m, 2H), 7.72-7.62 (m, 4H), 7.56-7.30 (m, 12H), 7.01 (d, *J* = 9.0 Hz, 2H), 6.76 (d, *J* = 3.1 Hz, 1H), 6.58 (dd, *J* = 3.3 Hz, 1.8 Hz, 1H). ^{13}C NMR (100 MHz, DMSO-d_6): δ = 156.72, 154.62, 150.00, 148.48, 143.28, 139.42, 133.55, 133.53, 132.26, 130.56, 129.72, 129.64, 128.70, 128.09, 127.66, 125.16, 120.58, 112.28, 107.18, 92.38. MS (MALDI-TOF, dithranol): *m/z* 549.32 for $C_{36}H_{25}N_2O_2S$ ($[M + H]^+$). Requires: 549.16. Anal. Calcd for $C_{36}H_{24}N_2O_2S$: C, 78.81; H, 4.41; N, 5.11; S, 5.84. Found: C, 78.55; H, 4.11; N, 5.44; S, 5.73.

Acknowledgments

The authors thank the Thuringian Ministry for Education, Science and Culture (grant #B514-09049, Photonische Mizellen [PhotoMIC]) for financial support.

Supplementary Material

Refinement data and X-ray structure file for **4a** and **C**, Picture of the betaines as solids and in solution (CH_3CN), linear correlation between the E_T(**X**) and E_T(**30**) values, Graphical representations of the NBO analysis, summary of the excited states in the UV region, ^{1}H and ^{13}C NMR spectra of the tetrafluoroborate salts and the betaines. Crystallographic data (excluding structure factors) has also been deposited with the Cambridge Crystallographic Data Centre as supplementary publication (CCDC-902653 for **4a** and CCDC-911688 for **C**). Copies of the data can be obtained free of charge on application to CCDC, 12 Union Road, Cambridge CB2 1EZ, UK or at www.ccdc.cam.ac.uk/data_request/cif.

References

1. Reichardt, C. *Chem. Soc. Rev.* **1992,** *21*, 147-153.
2. Dimroth, K.; Reichardt, C.; Siepmann, T.; Bohlmann, F. *Justus Liebigs Ann. Chem.* **1963,** *661*, 1-37.
3. Reichardt, C.; Che, D.; Heckenkemper, G.; Schäfer, G. *Eur. J. Org. Chem.* **2001,** *2001*, 2343-2361.
4. Reichardt, C. *Pure Appl. Chem.* **2008,** *80*, 1415-1432.
5. Reichardt, C. *Pure Appl. Chem.* **2004,** *76*, 1903-1919.
6. Reichardt, C.; Löbbecke, S.; Mehranpour, A. M.; Schäfer, G. *Can. J. Chem.* **1998,** *76*, 686-694.
7. Domínguez, M.; Rezende, M. C. *J. Phys. Org. Chem.* **2010,** *23*, 156-170.
8. Rezende, M. C.; Aracena, A. *Chem. Phys. Lett.* **2012,** *542*, 147-152.
9. Reichardt, C. *Solvents and solvent effects in organic chemistry*, 4th ed.; Wiley: New York, 2011.
10. Reichardt, C.; Eschner, M.; Schäfer, G. *J. Phys. Org. Chem.* **2001,** *14*, 737-751.
11. Langhals, H. *Anal. Lett.* **1990,** *23*, 2243-2258.
12. Ab Rani, M. A.; Brant, A.; Crowhurst, L.; Dolan, A.; Lui, M.; Hassan, N. H.; Hallett, J. P.; Hunt, P. A.; Niedermeyer, H.; Perez-Arlandis, J. M.; Schrems, M.; Welton, T.; Wilding, R. *Phys. Chem. Chem. Phys.* **2011,** *13*, 16831-16840.
13. Bolz, I.; Schaarschmidt, D.; Rüffer, T.; Lang, H.; Spange, S. *Angew. Chem. Int. Ed.* **2009,** *48*, 7440-7443.
14. Blum, P.; Mohr, G. J.; Matern, K.; Reichert, J.; Spichiger-Keller, U. E. *Anal. Chim. Acta* **2001,** *432*, 269-275.
15. Shekhovtsov, S. V.; McHedlov-Petrossyan, N. O.; Reichardt, C. *Tetrahedron Lett.* **2010,** *51*, 4347-4349.

16. McHedlov-Petrossyan, N. O.; Vodolazkaya, N. A.; Kornienko, A. A.; Karyakina, E. L.; Reichardt, C. *Langmuir* **2005,** *21*, 7090-7096.
17. Fidale, L.; Lima, P.; Hortêncio, L.; Pires, P.; Heinze, T.; El Seoud, O. *Cellulose* **2012,** *19*, 151-159.
18. Masternak, A.; Wenska, G.; Milecki, J.; Skalski, B.; Franzen, S. *J. Phys. Chem. A* **2005,** *109*, 759-66.
19. Happ, B.; Schaf̈er, J.; Menzel, R.; Hager, M. D.; Winter, A.; Popp, J.; Beckert, R.; Dietzek, B.; Schubert, U. S. *Macromolecules* **2011,** *44*, 6277-6287.
20. Menzel, R.; Ogermann, D.; Kupfer, S.; Weiß, D.; Görls, H.; Kleinermanns, K.; González, L.; Beckert, R. *Dyes Pigm.* **2012,** *94*, 512-524.
21. Calderón-Ortiz, L. K.; Täuscher, E.; Leite Bastos, E.; Görls, H.; Weiß, D.; Beckert, R. *Eur. J. Org. Chem.* **2012,** *2012*, 2535-2541.
22. Menzel, R.; Täuscher, E.; Weiß, D.; Beckert, R.; Görls, H. *Z. Anorg. Allg. Chem.* **2010,** *636*, 1380-1385.
23. Menzel, R.; Kupfer, S.; Mede, R.; Weiß, D.; Görls, H.; González, L.; Beckert, R. *Eur. J. Org. Chem.* **2012,** *2012*, 5231-5247.
24. Katritzky, A. R.; Manzo, R. H.; Lloyd, J. M.; Patel, R. C. *Angew. Chem. Int. Ed.* **1980,** *19*, 306-306.
25. Shekhovtsov, S. V.; Omelchenko, I. V.; Dyakonenko, V. V.; Shishkin, O. V.; Allmann, R.; Libor, T.; Reichardt, C.; McHedlov-Petrossyan, N. O. *Dyes Pigm.* **2012,** *92*, 1394-1399.
26. Milart, P.; Stadnicka, K. *Eur. J. Org. Chem.* **2001,** *2001*, 2337-2341.
27. Allmann, R. *Z. Krist.* **1969,** *128*, 115-132.
28. Täuscher, E.; Weiß, D.; Beckert, R.; Fabian, J.; Assumpção, A.; Görls, H. *Tetrahedron Lett.* **2011,** *52*, 2292-2294.
29. Kurjatschij, S.; Seichter, W.; Weber, E. *New J. Chem.* **2010,** *34*, 1465-1477.
30. Dean, J. A.; McGraw-Hill, 1999.
31. Kamlet, M. J.; Abboud, J. L. M.; Abraham, M. H.; Taft, R. W. *J. Org. Chem.* **1983,** *48*, 2877-2887.
32. Dimroth, K.; Reichardt, C. *Justus Liebigs Ann. Chem.* **1969,** *727*, 93-105.
33. Kolling, O. W. *Anal. Chem.* **1984,** *56*, 2988-2990.
34. Kamlet, M. J.; Taft, R. W. *JACS* **1976,** *98*, 377-383.
35. International Union of Pure and Applied Chemistry. Commission on Equilibrium Data.; Serjeant, E. P.; Dempsey, B.; International Union of Pure and Applied Chemistry. Commission on Electrochemical Data. *Ionisation constants of organic acids in aqueous solution*; Pergamon Press: Oxford ; New York, 1979.
36. Wojdyr, M. *J. Appl. Crystallogr.* **2010,** *43*, 1126-1128.
37. Reichardt, C. *Chem. Rev.* **1994,** *94*, 2319-2358.
38. Muller, P. *Pure Appl. Chem.* **1994,** *66*, 1077-1184.
39. Hofmann, K.; Schreiter, K.; Seifert, A.; Ruffer, T.; Lang, H.; Spange, S. *New J. Chem.* **2008,** *32*, 2180-2188.
40. El-Sayed, M.; Spange, S. *J. Phys. Chem. B* **2007,** *111*, 7224-7233.
41. Taft, R. W.; Abboud, J.-L. M.; Kamlet, M. J.; Abraham, M. H. *J. Solution Chem.* **1985,** *14*, 153-186.
42. Catalán, J.; Díaz, C. *Liebigs Ann.* **1997,** *1997*, 1941-1949.
43. Catalán, J. *J. Org. Chem.* **1997,** *62*, 8231-8234.
44. Catalán, J.; Palomar, J.; Díaz, C.; de Paz, J. L. G. *J. Phys. Chem. A* **1997,** *101*, 5183-5189.
45. Catalán, J. *J. Phys. Chem. B* **2009,** *113*, 5951-5960.
46. Aloise, S.; Pawlowska, Z.; Ruckebusch, C.; Sliwa, M.; Dubois, J.; Poizat, O.; Buntinx, G.; Perrier, A.; Maurel, F.; Jacques, P.; Malval, J.-P.; Poisson, L.; Piani, G.; Abe, J. *Phys. Chem. Chem. Phys.* **2012,** *14*, 1945-1956.
47. Runge, E.; Gross, E. K. U. *Phys. Rev. Lett.* **1984,** *52*, 997-1000.
48. Frisch, M. J.; Trucks, G. W.; Schlegel, H. B.; Scuseria, G. E.; Robb, M. A.; Cheeseman, J. R.; Scalmani, G.; Barone, V.; Mennucci, B.; Petersson, G. A.; Nakatsuji, H.; Caricato, M.; Li, X.; Hratchian, H. P.; Izmaylov, A. F.; Bloino, J.; Zheng, G.; Sonnenberg, J. L.; Hada, M.; Ehara, M.; Toyota, K.; Fukuda, R.; Hasegawa, J.; Ishida, M.; Nakajima, T.; Honda, Y.; Kitao, O.; Nakai, H.; Vreven, T.; Montgomery, J. A.; Peralta, J. E.; Ogliaro, F.; Bearpark, M.; Heyd, J. J.; Brothers, E.; Kudin, K. N.; Staroverov, V. N.; Kobayashi, R.; Normand, J.; Raghavachari, K.; Rendell, A.; Burant, J. C.; Iyengar, S. S.; Tomasi, J.; Cossi, M.; Rega, N.; Millam, J. M.; Klene, M.; Knox, J. E.; Cross, J. B.; Bakken, V.; Adamo, C.; Jaramillo, J.; Gomperts, R.; Stratmann, R. E.; Yazyev, O.; Austin, A. J.; Cammi, R.; Pomelli, C.; Ochterski, J. W.; Martin, R. L.; Morokuma, K.; Zakrzewski, V. G.; Voth, G. A.; Salvador, P.; Dannenberg, J. J.; Dapprich, S.; Daniels, A. D.; Farkas, O.; Foresman, J. B.; Ortiz, J. V.; Cioslowski, J.; Fox, D. J., Wallingford CT, 2009.
49. Becke, A. D. *J. Chem. Phys.* **1993,** *98*, 5648-5652.
50. Lee, C.; Yang, W.; Parr, R. G. *Phys. Rev. B* **1988,** *37*, 785-789.
51. Guthmuller, J.; Champagne, B. *J. Chem. Phys.* **2007,** *127*, 164507-11.
52. Becke, A. D. *Phys. Rev. A* **1988,** *38*, 3098-3100.
53. Harihara.Pc; Pople, J. A. *Theor. Chim. Acta* **1973,** *28*, 213-222.
54. Marder, S. R.; Perry, J. W.; Bourhill, G.; Gorman, C. B.; Tiemann, B. G.; Mansour, K. *Science* **1993,** *261*, 186-189.
55. Mennucci, B.; Cappelli, C.; Guido, C. A.; Cammi, R.; Tomasi, J. *J. Phys. Chem. A* **2009,** *113*, 3009-3020.
56. Cież, D.; Svetlik, J. *Synlett* **2011,** *3*, 315-318.
57. Täuscher, E.; Weiß, D.; Beckert, R.; Görls, H. *Synthesis* **2010,** *10*, 1603-1608.
58. Hooft, R. W. W. *COLLECT*; Nonius BV, Delft, The Netherlands, 1998.
59. Otwinowski, Z.; Minor, W. In *Methods Enzymol.;* Charles W. Carter, Jr. Ed.; Academic Press, 1997; pp. 307-326.
60. Sheldrick, G. *Acta Crystallogr., Sect. A: Found. Crystallogr.* **2008,** *64*, 112-122.